

# Analyzing Deep Neural Networks with Symbolic Propagation: Towards Higher Precision and Faster Verification

Pengfei Yang<sup>1,2</sup>, Jiangchao Liu<sup>3</sup>, Jianlin Li<sup>1,2</sup>, Liqian Chen<sup>3</sup>, and Xiaowei Huang<sup>4</sup>

<sup>1</sup> State Key Laboratory of Computer Science, Institute of Software, CAS, Beijing, China

<sup>2</sup> University of Chinese Academy of Sciences, Beijing, China

<sup>3</sup> National University of Defense Technology, Changsha, China

<sup>4</sup> Liverpool University, Liverpool, UK

**Abstract.** Deep neural networks (DNNs) have been shown lack of robustness for the vulnerability of their classification to small perturbations on the inputs. This has led to safety concerns of applying DNNs to safety-critical domains. Several verification approaches have been developed to automatically prove or disprove safety properties of DNNs. However, these approaches suffer from either the scalability problem, i.e., only small DNNs can be handled, or the precision problem, i.e., the obtained bounds are loose. This paper improves on a recent proposal of analyzing DNNs through the classic abstract interpretation technique, by a novel symbolic propagation technique. More specifically, the values of neurons are represented *symbolically* and propagated forwardly from the input layer to the output layer, on top of abstract domains. We show that our approach can achieve significantly higher precision and thus can prove more properties than using only abstract domains. Moreover, we show that the bounds derived from our approach on the hidden neurons, when applied to a state-of-the-art SMT based verification tool, can improve its performance. We implement our approach into a software tool and validate it over a few DNNs trained on benchmark datasets such as MNIST, etc.

## 1 Introduction

Deep neural networks (DNNs) have been broadly applied in various domains including nature language processing [1], image classification [11], game playing [22], etc. The performance of these DNNs, when measured with the prediction precision over a test dataset, is comparable to, or even better than, that of manually crafted software. However, for safety critical applications, it is required that the DNNs are certified against properties related to its safety. Unfortunately, DNNs have been found lack of robustness. Specifically, [23] discovers that it is possible to add a small, or even imperceptible, perturbation to a correctly classified input and make it misclassified. Such adversarial examples have raised serious concerns on the safety of DNNs. Consider a self-driving system controlled by a DNN. A failure on the recognition of a traffic light may lead to serious consequence because human lives are at stake.

Algorithms used to find adversarial examples are based on either gradient descent, see e.g., [23,2], or saliency maps, see e.g., [18], or evolutionary algorithm, see e.g.,

[17], etc. Roughly speaking, these are heuristic search algorithms without the guarantees to find the optimal values, i.e., the bound on the gap between an obtained value and its ground truth is unknown. However, the certification of a DNN needs provable guarantees. Thus, techniques based on formal verification have been developed. Up to now, DNN verifications include constraint-solving [19,10,13,7,15,27,5], layer-by-layer exhaustive search [9,26,25], global optimization [20], abstract interpretation [8], etc. Abstract interpretation is a theory of sound approximation of the semantics of programs [3], the basic idea of which is to use an abstract domain to over-approximate the computation on inputs. In [8], this idea has been developed for verifying DNNs. However, abstract interpretation can be imprecise, due to the non-linearity in DNNs.

The first contribution of this paper is to propose a novel symbolic propagation technique to enhance the precision of abstract interpretation based DNN verification. For every neuron, we *symbolically* represent, with an expression, how its value can be determined by the values of some neurons in previous layers. By both illustrative examples and experimental results, we show that, comparing with using only abstract domains, our new approach can find significantly tighter constraints over the neurons. Because abstract interpretation is a sound approximation, with tighter constraints, we may prove properties that cannot be proven by using only abstract domains. For example, we may prove a greater lower bound on the robustness of the DNNs.

Another contribution of this paper is to apply the value bounds derived from our approach on hidden neurons to improve the performance of a state-of-the-art SMT based DNN verifier Reluplex [10].

Finally, we implement our approach into a software tool<sup>5</sup> and validate it with a few DNNs trained on benchmark datasets such as MNIST, etc.

## 2 Preliminaries

We recall some basic notions on deep neural networks and abstract interpretation. For a vector  $\bar{x} \in \mathbb{R}^n$ , we use  $x_i$  to denote its  $i$ -th entry. For a matrix  $W \in \mathbb{R}^{m \times n}$ ,  $W_{i,j}$  denotes the entry in its  $i$ -th row and  $j$ -th column.

### 2.1 Deep neural networks

We work with deep feedforward neural networks, or DNNs, which can be represented as a function  $f : \mathbb{R}^m \rightarrow \mathbb{R}^n$ , mapping an input  $\bar{x} \in \mathbb{R}^m$  to its output  $\bar{y} = f(\bar{x}) \in \mathbb{R}^n$ . A DNN has in its structure a sequence of layers, including an input layer at the beginning, followed by several hidden layers, and an output layer in the end. Basically the output of a layer is the input of the next layer. The DNN  $f$  is the composition of the transformations between layers. Between two layers, typically a linear transformation followed by a non-linear activation function is performed. One of the most commonly used activation function is the rectified linear unit (ReLU) activation function, defined as

$$\text{ReLU}(x) = \max(x, 0)$$

---

<sup>5</sup> Available via Dropbox: <https://goo.gl/wLpQWj>

for  $x \in \mathbb{R}$  and  $\text{ReLU}(\bar{x}) = (\text{ReLU}(x_1), \dots, \text{ReLU}(x_n))$  for  $\bar{x} \in \mathbb{R}^n$ . We introduce the following three types of layers.

A **fully connected layer** is a function  $\text{FC}_{W, \bar{b}} : \mathbb{R}^m \rightarrow \mathbb{R}^n$ , such that  $W \in \mathbb{R}^{m \times n}$ ,  $\bar{b} \in \mathbb{R}^n$ , and

$$\text{FC}_{W, \bar{b}}(\bar{x}) = \text{ReLU}(W\bar{x} + \bar{b}).$$

A **convolutional layer**  $F^{p,q} = (F_1^{p,q}, \dots, F_t^{p,q})$  has a set of  $t$  filters such that  $p \leq m$  and  $q \leq n$ . Each filter  $F_l^{p,q} : \mathbb{R}^{m \times n \times r} \rightarrow \mathbb{R}^{(m-p+1) \times (n-q+1)}$ , parameterised over  $W \in \mathbb{R}^{p \times q \times r}$  and  $b \in \mathbb{R}$ , has its  $(i, j)$ -th entry  $F_l^{p,q}(\bar{x})_{i,j}$  as

$$\text{ReLU} \left( \sum_{i'=1}^p \sum_{j'=1}^q \sum_{k'=1}^r W_{i',j',k'} x_{i+i'-1, j+j'-1, k'} + b \right).$$

A **max pooling layer** takes as an input a three dimensional vector  $\bar{x} \in \mathbb{R}^{m \times n \times r}$ . With two parameters  $p$  and  $q$  which divides  $m$  and  $n$  respectively, we define  $\text{MaxPool}_{p,q}(\bar{x})_{i,j,k}$  as

$$\max\{x_{i',j',k} \mid p(i-1) < i' \leq pi, q(i-1) < j' \leq qi\}.$$

Let DNN  $f$  have  $N$  layers, each of which has  $m_k$  neurons, for  $0 \leq k < N$ . Therefore,  $m_0 = m$  and  $m_{N-1} = n$ .

## 2.2 Abstract interpretation

Abstract interpretation is a theory of sound approximation of the semantics of computer programs, which has been used in static analysis to verify properties of a program without actually running it. In the following, we describe its adaptation to work with DNNs.

Generally, on the input layer, we have a concrete domain  $\mathcal{C}$ , which includes a set of inputs  $X$  as one of its elements. To enable an efficient computation, we choose an abstract domain  $\mathcal{A}$  to infer the relation of variables in  $\mathcal{C}$ . We assume that there is a partial order  $\leq$  on  $\mathcal{C}$  as well as  $\mathcal{A}$ , which in our settings is the subset relation  $\subseteq$ .

**Definition 2.1.** A pair of functions  $\alpha : \mathcal{C} \rightarrow \mathcal{A}$  and  $\gamma : \mathcal{A} \rightarrow \mathcal{C}$  is a *Galois connection*, if for any  $a \in \mathcal{A}$  and  $c \in \mathcal{C}$ , we have  $\alpha(c) \leq a \Leftrightarrow c \leq \gamma(a)$ .

Intuitively, a Galois connection  $(\alpha, \gamma)$  expresses abstraction and concretization relations between domains, respectively. Note that,  $a \in \mathcal{A}$  is a sound abstraction of  $c \in \mathcal{C}$  if and only if  $c \leq \gamma(a)$ .

In abstract interpretation, it is important to choose a suitable abstract domain because it determines the efficiency and precision of the abstract interpretation. In practice, we use a certain type of constraints to represent the abstract elements. Geometrically, a certain type of constraints correspond to a special shape. E.g., the conjunction of a set of arbitrary linear constraints correspond to a polyhedron. Abstract domains that fit for verifying DNN include Intervals, Zonotopes, and Polyhedra.

- **Interval.** An interval  $I$  contains bound constraints in the form of  $a \leq x_i \leq b$ . The conjunction of bound constraints express a box in the Euclid space, and thus it is also named the Box abstract domain.
- **Zonotope.** A zonotope  $Z$  consists of constraints in the form of  $z_i = a_i + \sum_{j=1}^m b_{ij}\epsilon_j$ , where  $a_i, b_{ij}$  are real constants and  $\epsilon_j \in [l_j, u_j]$ . The conjunction of these constraints express a center-symmetric polyhedra in the Euclid space.
- **Polyhedra.** A Polyhedron  $P$  has constraints in the form of linear inequalities, i.e.  $\sum_{i=1}^n a_i x_i \leq b$  and it gives a closed convex polyhedron in the Euclid space.

*Example 2.2.* Let  $\bar{x} \in \mathbb{R}^2$ , and the range of  $\bar{x}$  be  $X = \{(1, 0), (0, 2), (1, 2), (2, 1)\}$ . With Interval, we can abstract the inputs  $X$  as  $[0, 2] \times [0, 2]$ , and with Zonotope,  $X$  can be abstracted as  $\{x_1 = 1 - \frac{1}{2}\epsilon_1 - \frac{1}{2}\epsilon_3, x_2 = 1 + \frac{1}{2}\epsilon_1 + \frac{1}{2}\epsilon_2\}$  where  $\epsilon_1, \epsilon_2, \epsilon_3 \in [-1, 1]$ . With Polyhedra,  $X$  can be abstracted as  $\{x_2 \leq 2, x_2 \leq -x_1 + 3, x_2 \geq x_1 - 1, x_2 \geq -2x_1 + 2\}$ .

### 3 Symbolic Propagation for Abstract Interpretation based DNN Verification

In this section, we first describe how to use abstract interpretation to verify DNNs. Then we present a symbolic propagation method to enhance its precision.

#### 3.1 Abstract interpretation based DNN verification

**The DNN verification problem** The problem of verifying DNNs can be stated formally as follows.

**Definition 3.1.** Given a function  $f : \mathbb{R}^m \rightarrow \mathbb{R}^n$  which expresses a DNN, a domain of the inputs  $X_0 \subseteq \mathbb{R}^m$ , and a property  $C \subseteq \mathbb{R}^n$ , it is to determine whether  $f(X_0) \subseteq C$  holds, where  $f(X_0) = \{f(\bar{x}) \mid \bar{x} \in X_0\}$ .

We use  $\|\bar{x} - \bar{x}_0\|_p$  with  $p \in [1, \infty]$  to denote the  $L_p$  norm distance between two vectors  $\bar{x}$  and  $\bar{x}_0$ . In this paper, we use  $L_\infty$  norm defined as follows.

$$\|\bar{x}\|_\infty = \max_{1 \leq i \leq n} |x_i|.$$

Note that, given an input  $\bar{x}_0 \in \mathbb{R}^m$  and a perturbation tolerance  $\delta > 0$ , the problem of verifying local robustness can be obtained by letting  $X_0$  be  $B(\bar{x}_0, \delta) := \{\bar{x} \mid \|\bar{x} - \bar{x}_0\|_p \leq \delta\}$  and  $C$  be  $C_L := \{\bar{y} \in \mathbb{R}^n \mid \arg \max_{1 \leq i \leq n} y_i = L\}$ , where  $L = \arg \max_{1 \leq i \leq n} f(\bar{x}_0)_i$  is the label of  $\bar{x}_0$ .

**Verifying DNNs via abstract interpretation** Under the framework of abstract interpretation, to conduct verification of DNNs, we first need to choose an abstract domain  $\mathcal{A}$ . Then we represent the set of inputs of a DNN as an abstract element (value)  $X_0^\sharp$  in  $\mathcal{A}$ . After that, we pass it through the DNN layers by applying abstract transformers of the abstract domain. Recall that  $N$  is the number of layers in a DNN and  $m_k$  is the number of nodes in the  $k$ -th layer. Let  $f_k$  (where  $1 \leq k < N$ ) be the layer function mapping from  $\mathbb{R}^{m_{k-1}}$  to  $\mathbb{R}^{m_k}$ . We can lift  $f_k$  to  $T_{f_k} : \mathcal{P}(\mathbb{R}^{m_k}) \rightarrow \mathcal{P}(\mathbb{R}^{m_k})$  such that  $T_{f_k}(X) = \{f_k(\bar{x}) \mid \bar{x} \in X\}$ .

**Definition 3.2.** An abstract transformer  $T_{f_k}^\sharp$  is a function mapping an abstract element  $X_{k-1}^\sharp$  in the abstract domain  $\mathcal{A}$  to another abstract element  $X_k^\sharp$ . Moreover,  $T_{f_k}^\sharp$  is sound if  $T_{f_k} \circ \gamma \subseteq \gamma \circ T_{f_k}^\sharp$ .

Intuitively, a sound abstract transformer  $T_{f_k}^\sharp$  maintains a sound relation between the abstract post-state and the abstract pre-state of a transformer in DNN (such as linear transformation, ReLU operation, etc.).

Let  $X_k = f_k(\dots(f_1(X_0)))$  be the exact set of resulting vectors in  $\mathbb{R}^{m_k}$  (i.e., the  $k$ -th layer) computed over the concrete inputs  $X_0$ , and  $X_k^\sharp = T_{f_k}^\sharp(\dots(T_{f_1}^\sharp(X_0^\sharp)))$  be the corresponding abstract value of the  $k$ -th layer when using an abstract domain  $\mathcal{A}$ . Note that  $X_0 \subseteq \gamma(X_0^\sharp)$ . We have the following conclusion.

**Proposition 1** If  $X_{k-1} \subseteq \gamma(X_{k-1}^\sharp)$ , then we have  $X_k \subseteq \gamma(X_k^\sharp) = \gamma \circ T_{f_k}^\sharp(X_{k-1}^\sharp)$ .

Therefore, when performing abstract interpretation over the transformations in a DNN, the abstract pre-state  $X_{k-1}^\sharp$  is transformed into abstract post-state  $X_k^\sharp$  by applying the abstract transformer  $T_{f_k}^\sharp$  which is built on top of an abstract domain. This procedure starts from  $k = 1$  and continues until reaching the output layer (and getting  $X_{N-1}^\sharp$ ). Finally, we use  $X_{N-1}^\sharp$  to check the property  $C$  as follows:

$$\gamma(X_{N-1}^\sharp) \subseteq C. \quad (1)$$

The following theorem states that this verification procedure based on abstract interpretation is sound for the DNN verification problem.

**Theorem 3.3.** If Equation (1) holds, then  $f(X_0) \subseteq C$ .

It's not hard to see that the other direction does not necessarily hold due to the potential incompleteness caused by the over-approximation made in both the abstract elements and the abstract transformers  $T_{f_k}^\sharp$  in an abstract domain.

*Example 3.4.* Let  $\bar{x}, \bar{y}, \bar{z} \in \mathbb{R}^2$ . Suppose that  $\bar{x}$  takes the value given in Example 1, and we have the following transformations:  $\bar{y} = \begin{pmatrix} 1 & 2 \\ 1 & -1 \end{pmatrix} \bar{x}$  and  $\bar{z} = \begin{pmatrix} 1 & 1 \\ -1 & 1 \end{pmatrix} \bar{y}$ . To cope with the above transformations, when using the Interval abstract domain, the resulting range of  $\bar{z}$  is  $([-2, 8] \ [-2, 8])^T$ , while using the Zonotope abstract domain, we get the resulting zonotope after the transformations as follows:

$$\left\{ z_1 = 3 - \frac{1}{2}\epsilon_1 + \frac{1}{2}\epsilon_2 - \epsilon_3, \quad z_2 = -3 - \frac{3}{2}\epsilon_1 - \frac{3}{2}\epsilon_2 \right\}.$$

The abstract value computed via abstract interpretation can be directly used to verify properties. Take the local robustness property, which expresses an invariance on the classification of  $f$  over a region  $B(\bar{x}_0, \delta)$ , as an example. Let  $l_i(\bar{x})$  be the confidence of  $\bar{x}$  being labeled as  $i$ , and  $l(\bar{x}) = \operatorname{argmax}_i l_i(\bar{x})$  be the label. It has been shown in [23,21] that DNNs are Lipschitz continuous. Therefore, when  $\delta$  is small, we have that  $|l_i(\bar{x}) - l_i(\bar{x}_0)|$  is also small for all labels  $i$ . That is, if  $l_i(\bar{x}_0)$  is significantly greater than  $l_j(\bar{x}_0)$  for  $j \neq i$ , it is highly likely that  $l_i(\bar{x})$  is also significantly greater than  $l_j(\bar{x})$ . It

is not hard to see that the more precise the relations among  $l_i(\bar{x}_0), l_i(\bar{x}), l_j(\bar{x}_0), l_j(\bar{x})$  computed via abstract interpretation, the more likely we can prove the robustness. Based on this reason, this paper aims to derive techniques to enhance the precision of abstract interpretation such that it can prove some more properties that cannot be proven by the original abstract interpretation.

### 3.2 Symbolic propagation for DNN verification

Symbolic propagation can ensure soundness while providing more precise results. In [24], a technique called symbolic interval propagation is present and we expand it to our abstraction interpretation framework so that it works on all abstract domains. First, we use the following example to show that using only abstract transformations in an abstract domain may lead to precision loss, while using symbolic propagation could enhance the precision.

*Example 3.5.* Assume that we have a two-dimensional input  $(x_1, x_2) \in [0, 1] \times [0, 1]$  and a few transformations  $y_1 := x_1 + x_2$ ,  $y_2 := x_1 - x_2$ , and  $z := y_1 + y_2$ . Suppose we use the Interval abstract domain to analyze the transformations.

- When using only the Interval abstract domain, we have  $y_1 \in [0, 2]$ ,  $y_2 \in [-1, 1]$ , and thus  $z \in [-1, 3]$  (i.e.,  $[0, 2] + [-1, 1]$ ).
- By symbolic propagation, we record  $y_1 = x_1 + x_2$  and  $y_2 = x_1 - x_2$  on the neurons  $y_1$  and  $y_2$  respectively, and then get  $z = 2x_1 \in [0, 2]$ . This result is more precise than that given by using only the Interval abstract domain.

Non-relational (e.g., intervals) or weakly-relational abstract domains (e.g., zones, octagons, zonotopes, etc.) [14] can not precisely encode the linear transformations (in the form of  $y := \sum_{i=1}^k w_i x_i + b$ ) in a DNN. Moreover, it is often the case for weakly-relational abstract domains that the composition of the optimal abstract transformers of individual statements in a sequence does not result in the optimal abstract transformer for the whole sequence, which has been shown in Example 3 when using only the interval abstract domain. A choice to precisely handle general linear transformations is to use the Polyhedra abstract domain which uses a conjunction of linear constraints as domain representation. However, the Polyhedra domain has the worst-case exponential space and time complexity when handling the ReLU operation (via the join operation in the abstract domain). As a consequence, DNN verification with the Polyhedra domain is impractical for large scale DNNs, which has been also confirmed in [8].

In this paper, we leverage symbolic propagation technique to enhance the precision for abstract interpretation based DNN verification. The insight behind is that linear transformations account for a large portion of the transformations in a DNN. Furthermore, when verifying properties such as robustness, the activation of a neuron can often be deterministic for inputs around an input with small perturbation. Hence, there should be a large number of linear equality relations that can be derived from the composition of a sequence of linear transformations via symbolic propagation. And we can use such linear equality relations to improve the precision of the results given by abstract domains. In Section 6, our experimental results confirm that, when the perturbation tolerance  $\delta$  is small, there is a significant proportion of neurons whose ReLU activations are consistent.

First, given  $X_0$ , a ReLU neuron  $y := \text{ReLU}(\sum_{i=1}^k w_i x_i + b)$  can be classified into one of the following 3 categories (according to its range information): (1) definitely-activated, if the range of  $\sum_{i=1}^k w_i x_i + b$  is a subset of  $[0, \infty)$ , (2) definitely-deactivated, if the range of  $\sum_{i=1}^k w_i x_i + b$  is a subset of  $(-\infty, 0]$ , and (3) uncertain, otherwise.

Now we detail our symbolic propagation technique. We first introduce a symbolic variable  $s_i$  for each node  $i$  in the input layer, to denote the initial value of that node. For a ReLU neuron  $d := \text{ReLU}(\sum_{i=1}^k w_i c_i + b)$  where  $c_i$  is a symbolic variable, we make use of the resulting abstract value of abstract domain at this node to determine whether the value of input of this node is definitely greater than 0 or definitely less than 0. If it is a definitely-activated neuron, we record for this neuron the linear combination  $\sum_{i=1}^k w_i c_i + b$  as its symbolic representation (i.e., the value of symbolic propagation). If it is a definitely-deactivated neuron, we record for this neuron the value 0 as its symbolic representation. Otherwise, we cannot have a linear combination as the symbolic representation and thus a fresh symbolic variable  $s_d$  is introduced to denote the output of this ReLU neuron. We also record the bounds for  $s_d$ , such that the lower bound for  $s_d$  is set to 0 (since the output of a ReLU neuron is always non-negative) and the upper bound keeps the one obtained by abstract interpretation.

To formalize the algorithm for ReLU node, we first define the abstract states in the analysis and three transfer functions for linear assignments, condition tests and joins respectively. An abstract state in our analysis is composed of an abstract element for a numeric domain (e.g., Box)  $\mathbf{n}^\# \in \mathbf{N}^\#$ , a set of free symbolic variables  $\mathbf{C}$  (those not equal to any linear expressions), a set of constrained symbolic variables  $\mathbf{S}$  (those equal to a certain linear expression), and a map from constrained symbolic variables to linear expressions  $\xi ::= \mathbf{S} \Rightarrow \{\sum_{i=1}^n a_i x_i + b \mid x_i \in \mathbf{C}\}$ . Note that we only allow free variables in the linear expressions in  $\xi$ . In the beginning, all input variables are taken as free symbolic variables. In Algorithm 1, we show the transfer functions for linear assignments  $[y := \sum_{i=1}^n a_i x_i + b]^\#$  which over-approximates the behaviors of  $y := \sum_{i=1}^n a_i x_i + b$ . If  $n > 0$  (i.e., the right value expression is not a constant), variable  $y$  is added to the constrained variable set  $\mathbf{S}$ . All constrained variables in  $\text{expr} = \sum_{i=1}^n a_i x_i + b$  is replaced by their corresponding expressions in  $\xi$ , and the map from  $y$  to the new  $\text{expr}$  is recorded in  $\xi$ . Abstract numeric element  $\mathbf{n}^\#$  is updated by the transfer function for assignments in the numeric domain  $[y := \text{expr}]_{\mathbf{N}^\#}^\#$ . If  $n \leq 0$ , the right-value expression is a constant, then  $y$  is added to  $\mathbf{C}$ , and is removed from  $\mathbf{S}$  and  $\xi$ .

The abstract transfer function for condition test is defined as  $[\text{expr} \leq 0]^\#(\mathbf{n}^\#, \mathbf{C}, \mathbf{S}, \xi) ::= ([\text{expr} \leq 0]_{\mathbf{N}^\#}^\#(\mathbf{n}^\#), \mathbf{C}, \mathbf{S}, \xi)$ , which only updates the abstract element  $\mathbf{n}^\#$  by the transfer function in the numeric domain  $\mathbf{N}^\#$ .

The join algorithm in our analysis is defined in Algorithm 2. Only the constrained variables arising in both input  $\mathbf{S}$ s and are with the same corresponding linear expressions are taken as constrained variables. The abstract element in the result is obtained by applying the join operator in the numeric domain  $\sqcup_{\mathbf{N}^\#}$ .

The transfer function for a ReLU node is defined as

$$[y := \text{ReLU}(\sum_{i=1}^k w_i x_i + b)]^\#(\mathbf{n}^\#, \mathbf{C}, \mathbf{S}, \xi) ::= \text{join}([y > 0]^\# \psi, [y := 0]^\#([y < 0]^\# \psi),$$

where  $\psi = [y := \sum_{i=1}^n a_i x_i + b]^\#(\mathbf{n}^\#, \mathbf{C}, \mathbf{S}, \xi)$ .

---

**Algorithm 1:** Transfer function for linear assignments  $[y := \sum_{i=1}^n a_i x_i + b]^\#$ 


---

**Input:** abstract numeric element  $\mathbf{n}^\# \in \mathbf{N}^\#$ , free variables  $\mathbf{C}$ , constrained variables  $\mathbf{S}$ , symbolic map  $\xi$

```

1 expr  $\leftarrow \sum_{i=1}^n a_i x_i + b$ 
2 When the right value expression just contains a constant
3 if  $n > 0$  then
4   for  $i \in [1, n]$  do
5     if  $x_i \in \mathbf{S}$  then
6       expr = expr $_{|x_i \leftarrow \xi(x_i)}$ 
7     end
8   end
9    $\xi = \xi \cup \{y \mapsto \mathbf{expr}\}$ 
10   $\mathbf{S} = \mathbf{S} \cup \{y\}$ 
11   $\mathbf{C} = \mathbf{C} / \{y\}$ 
12   $\mathbf{n}^\# = [y := \mathbf{expr}]_{\mathbf{N}^\#}^\#$ 
13 else
14    $\xi = \xi / (y \mapsto *)$ 
15    $\mathbf{C} = \mathbf{C} \cup \{y\}$ 
16    $\mathbf{S} = \mathbf{C} / \{y\}$ 
17    $\mathbf{n}^\# = [y := \mathbf{expr}]_{\mathbf{N}^\#}^\#$ 
18 end
19 end
20 return  $(\mathbf{n}^\#, \mathbf{C}, \mathbf{S}, \xi)$ 

```

---



---

**Algorithm 2:** Join algorithm **join**


---

**Input:**  $(\mathbf{n}_0^\#, \mathbf{C}_0, \mathbf{S}_0, \xi_0)$  and  $(\mathbf{n}_1^\#, \mathbf{C}_1, \mathbf{S}_1, \xi_1)$

```

1  $\mathbf{n}^\# = \mathbf{n}_0^\# \sqcup_{\mathbf{N}^\#} \mathbf{n}_1^\#$ 
2  $\xi = \xi_0 \cap \xi_1$ 
3  $\mathbf{S} = \{x \mid \exists \mathbf{expr}, x \rightarrow \mathbf{expr} \in \xi\}$ 
4  $\mathbf{C} = \mathbf{C}_0 \cup (\mathbf{S}_0 / \mathbf{S})$ 
5 return  $(\mathbf{n}^\#, \mathbf{C}, \mathbf{S}, \xi)$ 

```

---



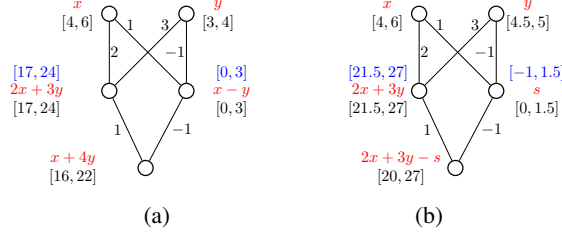


**Fig. 1.** An illustrative example of symbolic propagation

For a max pooling node  $d := \max_{1 \leq i \leq k} c_i$ , if there exists some  $c_j$  whose lower bound is larger than the upper bound of  $c_i$  for all  $i \neq j$ , we set  $c_j$  as the symbolic representation for  $d$ . Otherwise, we introduce a fresh symbolic variable  $s_d$  for  $d$  and record its bounds wherein its lower (upper) bound is the maximum of the lower (upper) bounds of  $c_i$ 's. Note that the lower (upper) bound of each  $c_i$  can be derived from the abstract value for this neuron given by abstract domain.

The algorithm for max-pooling layer can be defined with the three aforementioned transfer functions as follows:

$$\text{where } \phi_i = [d := c_i]^\# [c_i \geq c_1]^\# \dots [c_i \geq c_k]^\# (\mathbf{n}^\#, \mathbf{C}, \mathbf{S}, \xi)$$

*Example 3.6.* For the DNN shown in Figure 1(a), there are two input nodes denoted by symbolic variables  $x$  and  $y$ , two hidden nodes, and one output node. The initial ranges of the input symbolic variables  $x$  and  $y$  are given, i.e.,  $[4, 6]$  and  $[3, 4]$  respectively. The weights are labeled on the edges. It is not hard to see that, when using the Interval abstract domain, (the inputs of) the two hidden nodes have bounds  $[17, 24]$  and  $[0, 3]$  respectively. For the hidden node with  $[17, 24]$ , we know that this ReLU node is definitely activated, and thus we use symbolic propagation to get a symbolic expression  $2x + 3y$  to symbolically represent the output value of this node. Similarly, for the hidden node with  $[0, 3]$ , we get a symbolic expression  $x - y$ . Then for the output node, symbolic propagation results in  $x + 4y$ , which implies that the output range of the whole DNN is  $[16, 22]$ . If we use only the Interval abstract domain without symbolic propagation, we will get the output range  $[14, 24]$ , which is less precise than  $[16, 22]$ .

For the DNN shown in Figure 1(b), we change the initial range of the input variable  $y$  to be  $[4.5, 5]$ . For the hidden ReLU node with  $[-1, 1.5]$ , it is neither definitely activated nor definitely deactivated, and thus we introduce a fresh symbolic variable  $s$  to denote the output of this node, and set its bound to  $[0, 1.5]$ . For the output node, symbolic propagation results in  $2x + 3y - s$ , which implies that the output range of the whole DNN is  $[20, 27]$ .

For a definitely-activated neuron, we utilize its symbolic representation to enhance the precision of abstract domains. We add the linear constraint  $d == \sum_{i=1}^k w_i c_i + b$  into the abstract value at (the input of) this node, via the meet operation (which is used to deal with conditional test in a program) in the abstract domain [3]. If the precision of the abstract value for the current neuron is improved, we may find more definitely-activated

neurons in the subsequent layers. In other words, the analysis based on abstract domain and our symbolic propagation mutually improves the precision of each other on-the-fly.

After obtaining symbolic representation for all the neurons in a layer  $k$ , the computation proceeds to layer  $k + 1$ . The computation terminates after completing the computation for the output layer. All symbolic representations in the output layer are evaluated to obtain value bounds.

The following theorem shows some results on precision of our symbolic propagation technique.

**Theorem 3.7.** (1) For an FNN  $f : \mathbb{R}^m \rightarrow \mathbb{R}^n$  and a box region  $X \subseteq \mathbb{R}^m$ , the Box abstract domain with symbolic propagation can give a more precise abstraction for  $f(X)$  than the Zonotope abstract domain without symbolic propagation.

(2) For an FNN  $f : \mathbb{R}^m \rightarrow \mathbb{R}^n$  and a box region  $X \subseteq \mathbb{R}^m$ , the Box abstract domain with symbolic propagation and the Zonotope abstract domain with symbolic propagation gives the same abstraction for  $f(X)$ .

(3) There exists a CNN  $g : \mathbb{R}^m \rightarrow \mathbb{R}^n$  and a box region  $X \subseteq \mathbb{R}^m$  s.t. the Zonotope abstract domain with symbolic propagation give a strictly more precise abstraction for  $g(X)$  than the Box abstract domain with symbolic propagation.

*Proof.* (1) It suffices to consider the ReLU nodes because Neither Box with symbolic propagation nor Zonotope without symbolic propagation does not lose precision in linear transformations. Let  $X'$  be a zonotope region, and we consider  $\text{ReLU}(X')$ . First we consider Box with symbolic propagation. For a definitely activated node  $y_i$ , it will keep its symbolic representation. For a definitely deactivated node  $y_i$ , its symbolic representation is  $y_i = 0$ . For an uncertain node  $y_i$ , we will build a new symbol for it and record its range. The abstraction of  $\bar{y}$  consists of these symbol representations, and it represents the cylinder with the precise zonotope of the activated dimensions and the deactivated dimensions as the base and the uncertain dimensions along with their ranges as the cylindrical surface. Now we consider Zonotope. Compared with Box with symbolic propagation, Zonotope has the same precision on definitely activated and deactivated nodes. However, when Zonotope deals with uncertain nodes, it has a join operation and destroys all the relations among them, so it loses more precision than Box with symbolic propagation.

(2) Box or Zonotope with symbolic propagation does not lose precision in linear transformations from the algorithm of symbolic propagation and the linear transformations for Zonotope, so it suffices to show that Zonotope with symbolic propagation does not give a more precise abstraction on ReLU nodes. For the activated and deactivated nodes, obviously they have the same precise abstraction. For the uncertain nodes, as (1) shows, zonotope cannot preserve relations for these nodes, and it behaves as Box does.

(3) Let the zonotope  $X' = \{x_1 = 2 + \epsilon_1 + \epsilon_2, x_2 = 2 + \epsilon_1 - \epsilon_2 \mid \epsilon_1, \epsilon_2 \in [-1, 1]\}$  and the max pooling node  $y = \max\{x_1, x_2\}$ . Obviously  $X'$  can be obtained through a linear transformation on some box region  $X$ . With Box with symbolic propagation, the abstraction of  $y$  is  $[0, 4]$ , while Zonotope with symbolic propagation gives the abstraction is  $[1, 4]$ .

Thm 3.7 gives us some insights: Symbolic propagation technique has a very strong power (even stronger than Zonotope) in dealing with ReLU nodes, while Zonotope

gives a more precise abstraction on max pooling nodes. It also provides a useful instruction: When we work with FNNs with the input range being an interval, we should use Interval with symbolic propagation rather than Zonotope with symbolic propagation since it does not improve the precision but takes more time. Results in Thm 3.7 will also be illustrated in our experiments.

## 4 Abstract Interpretation as an Accelerator for SMT based DNN Verification

In this section we briefly recall DNN verification based on SMT solvers, and then describe how to utilize the results by abstract interpretation with our symbolic propagation to improve its performance.

### 4.1 SMT based DNN verification

In [10,7], two SMT solvers Reluplex and Planet were presented to verify DNNs. Typically an SMT solver combines a SAT solver with specialized decision procedures for other theories. The verification of DNNs uses linear arithmetic over real numbers, in which an atom may have the form of  $\sum_{i=1}^n a_i x_i \leq b$ , where  $a_i$  and  $b$  are real numbers. Both Reluplex and Planet use the DPLL algorithm to split cases and rule out conflict clauses. They are different in dealing with the intersection. For Reluplex, it inherits rules from the Simplex algorithm and adds a few rules dedicated to ReLU operation. Through the classical pivot operation, it searches for a solution to the linear constraints, and then apply the rules for ReLU to ensure the ReLU relation for every node. Differently, Planet uses linear approximation to over-approximate the DNN, and manage the conditions of ReLU and max pooling nodes with logic formulas.

### 4.2 Abstract interpretation with symbolic propagation as an accelerator

SMT-based DNN verification approaches are often not efficient, e.g., relying on case splitting for ReLU operation. In the worst case, case splitting is needed for each ReLU operation in a DNN. In particular, when analyzing large-scale DNNs, SMT-based DNN verification approaches may suffer from the scalability problem and account time out, which is also confirmed experimentally in [8].

In this paper, we utilize the results of abstract interpretation (with symbolic propagation) to accelerate SMT-based DNN verification approaches. More specifically, we use the bound information of each ReLU node (obtained by abstract interpretation) to reduce the number of case-splitting, and thus accelerate SMT-based DNN verification. For example, on a neuron  $d := \text{ReLU}(\sum_{i=1}^k w_i c_i + b)$ , if we know that this node is a definitely-activated node according to the bounds given by abstract interpretation, we only consider the case  $d := \sum_{i=1}^k w_i c_i + b$  and thus no split is applied. We remark that, this does not compromise the precision of SMT-based DNN verification while improving their efficiency.

## 5 Discussion

In this section, we discuss the soundness guarantee of our approach. Soundness is a very desirable property of formal verification.

Abstract interpretation is known for its soundness guarantee for analysis and verification [14], since it conducts over-approximation to enclose all the possible behaviors of the original system. Computing over-approximations for a DNN is thus our soundness guarantee in this paper. As shown in Theorem 3.3, if the results of abstract interpretation show that the property  $C$  holds (i.e.,  $\gamma(X^\sharp_N) \subseteq C$  in Equation 1), then the property also holds for the set of actual executions of the DNN (i.e.,  $f(X_0) \subseteq C$ ). If the results of abstract interpretation can not prove that the property  $C$  holds, however, the verification is inconclusive. In this case, the results of the chosen abstract domain are not precise enough to prove the property, and thus more powerful abstract domains are needed. Moreover, our symbolic propagation also preserves soundness, since it uses symbolic substitution to compute the composition of linear transformations.

On the other hand, many existing DNN verification tools do not guarantee soundness. For example, Reluplex [10] (using GLPK), Planet [7] (using GLPK), and Sherlock [4] (using Gurobi) all rely on the floating point implementation of linear programming solvers, which is unsound. Actually, most state-of-the-art linear programming solvers use floating-point arithmetic and only give approximate solutions which may not be the actual optimum solution or may even lie outside the feasible space [16]. It may happen that a linear programming solver implemented via floating point arithmetic wrongly claims that a feasible linear system is infeasible or the other way round. In fact, [4] reports several false positive results in Reluplex, and mentions that this comes from unsound floating point implementation.

## 6 Experimental Evaluation

We present the design and results of our experiment.

### 6.1 Experimental setup

**Dataset and DNNs** We use the MNIST dataset [12], which contains 60,000  $28 \times 28$  grayscale handwritten digits. On MNIST, we train seven FNNs (i.e., DNNs with only fully-connected layers), and one CNN (i.e., DNNs with fully-connected, convolutional, and max-pooling layers). The seven FNNs are of the size  $3 \times 20$ ,  $6 \times 20$ ,  $3 \times 50$ ,  $3 \times 100$ ,  $6 \times 100$ , and  $9 \times 200$ , where  $m \times n$  refers to  $m$  hidden layers with  $n$  neurons in each hidden layer. The CNN consists of 2 convolutional, 1 max pooling, 2 convolutional, 1 max-pooling, and 3 fully connected layers in sequence.

**Properties.** We consider the local robustness property with respect to the  $L_\infty$ -norm. Formally, for networks on MNIST we set the input region as

$$S_{\bar{x}, \delta} = \{\bar{x}' \in \mathbb{R}^m \mid \forall i. 1 - \delta \leq x_i \leq x'_i \leq 1 \vee x_i = x'_i\}.$$

In the experiments for MNIST, the optional robustness bound  $\delta \in \{0.1, 0.4, 0.6\}$ .

Experiments are conducted on an openSUSE Leap 15.0 machine with Intel i7 CPU@3.60GHz and 16GB memory.

	Box	Zono	SymBox	SymZono	Planet
FNN1	-24.63 17.30	-13.10 5.526	-6.771 -0.502	-6.771 -0.502	-5.659 -2.118
FNN2	-116.3 116.4	-90.07 89.53	-12.81 2.418	-12.81 2.418	-6.675 -4.304
FNN3	-46.99 31.51	-32.15 11.62	-13.84 -5.626	-13.84 -5.626	-11.73 -8.411
FNN4	-46.24 47.34	-28.12 24.01	-10.63 1.753	-10.63 1.753	-5.636 -3.630
FNN5	-1200 1144	-932.7 887.0	-386.3 365.5	-386.3 365.5	-14.46 -1.434
FNN6	-3669 4052	-2805 3096	-1035 1149	-1035 1149	-111.5 121.1
FNN7	-206814 231106	-189630 211903	-70992 79330	-70992 79330	TIMEOUT
CNN	-527.2 463.2	-205.8 167.0	-254.3 213.4	-94.69 64.93	TIMEOUT

(a)

	Box	Zono	SymBox	SymZono	Planet
FNN1	11.168 0.2	13.482 0.5	12.935 0.6	17.144 0.6	20.179 0.6
FNN2	12.559 0	16.636 0.2	15.075 0.5	22.333 0.5	35.84 0.6
FNN3	12.699 0.2	18.748 0.3	19.042 0.6	28.128 0.6	76.106 0.6
FNN4	15.583 0.1	29.495 0.3	37.716 0.6	56.47 0.6	351.139 0.6
FNN5	28.963 0	81.49 0.2	90.208 0.4	154.222 0.4	1297.485 0.6
FNN6	62.766 0	398.565 0.1	323.328 0.3	650.629 0.3	15823.208 0.3
FNN7	111.955 0	1674.465 0	642.978 0.3	1524.975 0.3	TIMEOUT
CNN	2340.828 0	6717.57 0.2	5124.681 0.2	8584.555 0.3	TIMEOUT

(b)

	Box	Zono	SymBox	SymZono	Planet
FNN1(60)	57 44 34	59 52 38	59 53 44	59 53 44	59 56 55
FNN2(120)	103 59 38	118 109 66	118 113 107	118 113 107	119 114 110
FNN3(150)	136 93 66	141 127 85	143 133 110	143 133 110	146 142 135
FNN4(300)	250 144 105	294 209 130	295 254 182	295 254 182	296 276 254
FNN5(600)	289 160 106	513 200 125	589 510 236	589 510 236	593 558 493
FNN6(1200)	472 247 181	782 339 195	1176 790 250	1176 790 250	1189 1089 772
FNN7(1800)	469 271 177	770 350 200	1773 741 263	1773 741 263	TIMEOUT
CNN(12412)	12226 11788 11280	12371 12119 11786	12373 12094 11659	12376 12193 11877	TIMEOUT

(c)

**Fig. 2.** Experimental results: (a) The lower and upper bounds of the 8-th entry in the output layer (corresponding to the classification of the number 7) with the robustness bound  $\delta = 0.6$ , and the fixed input Picture 1955; (b) The time (in second) and the maximum robustness bound  $\delta$  which can be verified through the abstract interpretation technique and the planet bound, with optional  $\delta \in \{0.1, 0.2, 0.3, 0.4, 0.5, 0.6\}$ , and the fixed input Picture 2090; (c) The number of hidden ReLU neurons whose behavior can be decided with the bounds our abstract interpretation technique and Planet provide with optional robustness bound  $\delta \in \{0.1, 0.4, 0.6\}$ , and the fixed input Picture 767.

## 6.2 Experimental Results

We compare five approaches: Box, Zono, SymBox, SymZono, and Planet. Box and Zono are baseline approaches of abstract interpretation with abstract domain as Interval and Zonotope, respectively. SymBox and SymZone are our enhanced abstract interpretation with symbolic propagation, for abstract domain as Interval and Zonotope, respectively. Planet serves as the benchmark verification approach (for its ability to compute bounds).

*Improvement on Bounds* To see the improvement on bounds, we fix an input  $\bar{x}$  and a tolerance  $\delta$ , and use the above five approaches to generate bounds for a given output label. Figure 3(a) reports the results on an input  $\bar{x}$  (No. 1955 in the MNIST training dataset) and a tolerance  $\delta = 0.6$ . In all our experiments, we set TIMEOUT as one hour for a single run with a DNN, an input, and a tolerance  $\delta$ . In Figure 3(a), every entry contains two numbers, for the lower and upper bound of the 8-th label, respectively. We can see that, in general, SymBox and SymZono can achieve much better bounds than Box and Zono do. These bounds are close to Planet has, except for FNN5 and FNN6. On the other hand, while SymBox and SymZone can still return in a reasonable time, Planet cannot return in a hour for FNN7 and CNN, which have 1800 and 12412 hidden neurons, respectively. Results in Thm 3.7 are all illustrated here.

*Greater Verifiable Robustness Bounds* Figure 3(b) shows the results of using the obtained bounds to do robustness verification. We consider a few thresholds for robustness

tolerance, i.e.,  $\{0.1, 0.4, 0.6\}$ , and find that SymBox and SymZono can achieve much greater bounds than Box and Zono do, and moreover their bounds are the same as or close to what Planet can do.

*Proportion of Activated/Deactivated ReLU Nodes* Figure 3(c) reports the number of hidden neurons whose ReLU behaviour (i.e., activated or deactivated) has been consistent within the tolerance  $\delta$ . Comparing with Box and Zono, our SymBox and SymZono can confirm the ReLU behaviour with a much higher percentage.

*Faster Verification* To evaluate the benefits of tighter value bounds for SMT based tools, we give the bounds by abstract interpretation (on Box domain with symbolic propagation) to Reluplex [10] and observe the performance difference. The results are shown in Table 1. Each cell shows the satisfiability (i.e., SAT if an adversarial example is found) or the running time without or with given bounds. The experiments are conducted on different  $\delta$  values [10] and a fixed network (nnet1\_1) and 5 fixed points (Point 1 to 5 in [10]). The time our technique spent on deriving the bounds are all less than 1 second. Table 1 shows that tighter initial bounds bring significant benefits to Reluplex with an overall  $(\frac{1}{5076} - \frac{1}{32992}) / \frac{1}{32992} = 549.43\%$  speedup (9.16 hours compared to 1.41 hours). However, it should be noted that, on one specific case (i.e.,  $\delta = 0.1$  at Point 1), the tighter initial bounds slow Reluplex, which means that the speedup is not guaranteed on all cases.

		$\delta = 0.1$		$\delta = 0.075$		$\delta = 0.05$		$\delta = 0.025$		$\delta = 0.01$		Total Time
		Result	Time	Result	Time	Result	Time	Result	Time	Result	Time	
Point 1	Reluplex	SAT	39	SAT	123	SAT	14	UNSAT	638	UNSAT	64	879
	Reluplex + ABS	SAT	45	SAT	36	SAT	14	UNSAT	237	UNSAT	36	368
Point 2	Reluplex	UNSAT	6513	UNSAT	1559	UNSAT	319	UNSAT	49	UNSAT	11	8451
	Reluplex + ABS	UNSAT	141	UNSAT	156	UNSAT	75	UNSAT	40	UNSAT	0	412
Point 3	Reluplex	UNSAT	1013	UNSAT	422	UNSAT	95	UNSAT	79	UNSAT	6	1615
	Reluplex + ABS	UNSAT	44	UNSAT	71	UNSAT	0	UNSAT	0	UNSAT	0	115
Point 4	Reluplex	SAT	3	SAT	5	SAT	1236	UNSAT	579	UNSAT	8	1831
	Reluplex + ABS	SAT	3	SAT	7	UNSAT	442	UNSAT	31	UNSAT	0	483
Point 5	Reluplex	UNSAT	14301	UNSAT	4248	UNSAT	1392	UNSAT	269	UNSAT	6	20216
	Reluplex + ABS	UNSAT	2002	UNSAT	1402	UNSAT	231	UNSAT	63	UNSAT	0	3698

**Table 1.** The satisfiability on given  $\delta$ , and the times (in second) with and without bounds generated by abstract interpretation with symbolic propagation on the BOX domain.

## 7 Related Work

Verification of neural networks can be traced back to [19], where the network is encoded after approximating every sigmoid activation function with a set of piecewise linear constraints and then solved with an SMT solver. It works with a network of 6 hidden nodes. More recently, by considering DNNs with ReLU activation functions,

the verification approaches include constraint-solving [10,13,7,15], layer-by-layer exhaustive search [9,26], global optimisation [20], abstract interpretation [8], etc. More specifically, [10] presents an SMT solver Reluplex to verify properties on DNNs with fully-connected layers. [7] presents another SMT solver Planet which combines linear approximation and interval arithmetic to work with fully connected and max pooling layers. Methods based on SMT solvers do not scale well, e.g., Reluplex can only work with DNNs with about a few hidden neurons.

Besides the verification problem, research has been conducted on the output range problem. In [4], Sherlock, an algorithm based on local and global search and mixed integer linear programming (MILP), is put forward to calculate the output range of a given label when the inputs are restricted to a small subspace. It is shown that Sherlock is much more efficient in calculating output range than Reluplex. [20] also gives an algorithm for output range analysis, and their algorithm is workable for all Lipschitz continuous DNNs, including all layers and activation functions mentioned above. In [24], the authors use symbolic interval propagation to calculate output range. Compared with this work, our approach is sound and fits for general abstract domains, while their symbolic interval propagation is unsound (see Sect. 5) and is designed specifically for symbolic intervals.

[8] is the first to use abstract interpretation to verify DNNs. They define a class of functions called conditional affine transformations (CAT) to characterize DNNs containing fully connected, convolutional and max pooling layers with the ReLU activation function. They use Interval and Zonotope as the abstract domains and the powerset technique on Zonotope. The performance of their tool AI<sup>2</sup> is much more effective than Reluplex. Compared with this work, we use symbolic propagation rather than powerset extension techniques to enhance the precision of abstract interpretation based DNN verification. Symbolic propagation is more lightweight than powerset extension. Moreover, we also use the bounds information given by abstract interpretation to accelerate SMT based DNN verification.

## 8 Conclusion

In this paper, we enhance the abstract interpretation based DNN verification approach with a symbolic propagation technique. We show theoretically and experimentally that this new technique can improve the bounds and speed up the verification procedure.

## References

1. Deep neural networks for acoustic modeling in speech recognition: The shared views of four research groups. *IEEE Signal Process. Mag.* 29(6), 82–97 (2012), <https://doi.org/10.1109/MSP.2012.2205597>
2. Carlini, N., Wagner, D.: Towards evaluating the robustness of neural networks. In: *Security and Privacy (SP)*, 2017 IEEE Symposium on. pp. 39–57. IEEE (2017)
3. Cousot, P., Cousot, R.: Abstract interpretation: A unified lattice model for static analysis of programs by construction or approximation of fixpoints. In: *Fourth ACM Symposium on Principles of Programming Languages (POPL)*. pp. 238–252 (1977)

4. Dutta, S., Jha, S., Sankaranarayanan, S., Tiwari, A.: Output range analysis for deep feedforward neural networks. In: Dutle, A., Muñoz, C.A., Narkawicz, A. (eds.) *NASA Formal Methods - 10th International Symposium, NFM 2018*, Newport News, VA, USA, April 17-19, 2018, *Proceedings. Lecture Notes in Computer Science*, vol. 10811, pp. 121–138. Springer (2018), [https://doi.org/10.1007/978-3-319-77935-5\\_9](https://doi.org/10.1007/978-3-319-77935-5_9)
5. Dvijotham, K., Stanforth, R., Gopal, S., Mann, T.A., Kohli, P.: A dual approach to scalable verification of deep networks. *CoRR abs/1803.06567* (2018), <http://arxiv.org/abs/1803.06567>
6. Dy, J.G., Krause, A. (eds.): *Proceedings of the 35th International Conference on Machine Learning, ICML 2018, Stockholm, Sweden, July 10-15, 2018, JMLR Workshop and Conference Proceedings*, vol. 80. JMLR.org (2018), <http://proceedings.mlr.press/v80/>
7. Ehlers, R.: Formal verification of piece-wise linear feed-forward neural networks. In: *15th International Symposium on Automated Technology for Verification and Analysis (ATVA2017)*. pp. 269–286 (2017)
8. Gehr, T., Mirman, M., Drachler-Cohen, D., Tsankov, P., Chaudhuri, S., Vechev, M.: AI<sup>2</sup>: Safety and robustness certification of neural networks with abstract interpretation. In: *2018 IEEE Symposium on Security and Privacy (S&P 2018)*. pp. 948–963 (2018)
9. Huang, X., Kwiatkowska, M., Wang, S., Wu, M.: Safety verification of deep neural networks. In: *29th International Conference on Computer Aided Verification (CAV2017)*. pp. 3–29 (2017)
10. Katz, G., Barrett, C.W., Dill, D.L., Julian, K., Kochenderfer, M.J.: Reluplex: An efficient SMT solver for verifying deep neural networks. In: *29th International Conference on Computer Aided Verification (CAV2017)*. pp. 97–117 (2017)
11. Krizhevsky, A., Sutskever, I., Hinton, G.E.: Imagenet classification with deep convolutional neural networks. In: Bartlett, P.L., Pereira, F.C.N., Burges, C.J.C., Bottou, L., Weinberger, K.Q. (eds.) *Advances in Neural Information Processing Systems 25: 26th Annual Conference on Neural Information Processing Systems 2012. Proceedings of a meeting held December 3-6, 2012, Lake Tahoe, Nevada, United States*. pp. 1106–1114 (2012), <http://papers.nips.cc/paper/4824-imagenet-classification-with-deep-convolutional-neural-networks>
12. LéCun, Y., Bottou, L., Bengio, Y., Haffner, P.: Gradient-based learning applied to document recognition. *Proceedings of the IEEE* 86(11), 2278–2324 (1998)
13. Lomuscio, A., Maganti, L.: An approach to reachability analysis for feed-forward ReLU neural networks. In: *KR2018* (2018)
14. Miné, A.: Tutorial on static inference of numeric invariants by abstract interpretation. *Foundations and Trends in Programming Languages* 4(3-4), 120–372 (2017)
15. Narodytska, N., Kasiviswanathan, S.P., Ryzhyk, L., Sagiv, M., Walsh, T.: Verifying properties of binarized deep neural networks. *arXiv preprint arXiv:1709.06662* (2017)
16. Neumaier, A., Shcherbina, O.: Safe bounds in linear and mixed-integer linear programming. *Math. Program.* 99(2), 283–296 (2004)
17. Nguyen, A., Yosinski, J., Clune, J.: Deep neural networks are easily fooled: High confidence predictions for unrecognizable images. In: *Proceedings of the IEEE Conference on Computer Vision and Pattern Recognition*. pp. 427–436 (2015)
18. Papernot, N., McDaniel, P.D., Jha, S., Fredrikson, M., Celik, Z.B., Swami, A.: The limitations of deep learning in adversarial settings. *CoRR abs/1511.07528* (2015), <http://arxiv.org/abs/1511.07528>
19. Pulina, L., Tacchella, A.: An abstraction-refinement approach to verification of artificial neural networks. In: Touili, T., Cook, B., Jackson, P.B. (eds.) *Computer Aided Verification, 22nd International Conference, CAV 2010, Edinburgh, UK, July 15-19, 2010. Pro-*



- ceedings. Lecture Notes in Computer Science, vol. 6174, pp. 243–257. Springer (2010), [https://doi.org/10.1007/978-3-642-14295-6\\_24](https://doi.org/10.1007/978-3-642-14295-6_24)
20. Ruan, W., Huang, X., Kwiatkowska, M.: Reachability analysis of deep neural networks with provable guarantees. In: Lang, J. (ed.) Proceedings of the Twenty-Seventh International Joint Conference on Artificial Intelligence, IJCAI 2018, July 13–19, 2018, Stockholm, Sweden. pp. 2651–2659. ijcai.org (2018), <https://doi.org/10.24963/ijcai.2018/368>
  21. Ruan, W., Huang, X., Kwiatkowska, M.: Reachability analysis of deep neural networks with provable guarantees. In: IJCAI2018. pp. 2651–2659 (2018)
  22. Silver, D., Huang, A., Maddison, C.J., Guez, A., Sifre, L., van den Driessche, G., Schrittwieser, J., Antonoglou, I., Panneershelvam, V., Lanctot, M., Dieleman, S., Grewe, D., Nham, J., Kalchbrenner, N., Sutskever, I., Lillicrap, T.P., Leach, M., Kavukcuoglu, K., Graepel, T., Hassabis, D.: Mastering the game of go with deep neural networks and tree search. *Nature* 529(7587), 484–489 (2016), <https://doi.org/10.1038/nature16961>
  23. Szegedy, C., Zaremba, W., Sutskever, I., Bruna, J., Erhan, D., Goodfellow, I., Fergus, R.: Intriguing properties of neural networks. In: International Conference on Learning Representations (ICLR2014) (2014)
  24. Wang, S., Pei, K., Whitehouse, J., Yang, J., Jana, S.: Formal security analysis of neural networks using symbolic intervals. CoRR abs/1804.10829 (2018), <http://arxiv.org/abs/1804.10829>
  25. Weng, T., Zhang, H., Chen, H., Song, Z., Hsieh, C., Daniel, L., Boning, D.S., Dhillon, I.S.: Towards fast computation of certified robustness for relu networks. In: Dy and Krause [6], pp. 5273–5282, <http://proceedings.mlr.press/v80/weng18a.html>
  26. Wicker, M., Huang, X., Kwiatkowska, M.: Feature-guided black-box safety testing of deep neural networks. In: International Conference on Tools and Algorithms for the Construction and Analysis of Systems (TACAS2018). pp. 408–426. Springer (2018)
  27. Wong, E., Kolter, J.Z.: Provable defenses against adversarial examples via the convex outer adversarial polytope. In: Dy and Krause [6], pp. 5283–5292, <http://proceedings.mlr.press/v80/wong18a.html>